



INTEGRATED STRATIGRAPHIC AND PETROPHYSICAL ASSESSMENT OF THE MADUKY FIELD, NIGER DELTA, NIGERIA: IMPLICATIONS FOR RESERVOIR ARCHITECTURE AND HYDROCARBON PROSPECTIVITY

Samuel Okechukwu Onyekuru ¹ , Reginald Chinonso Maduka ¹, Timothy Chibuikwe Anyanwu ¹ , Ikechukwu Onyema Njoku ¹, Diugo Okereke Ikoro ¹, Chinyere Caroline Amadi ¹, Okechukwu Ebuka Agbasi ² , Victor Inumidun Fagorite ³

¹ Department of Geology, Federal University of Technology, P.M.B. 1526, Owerri-Nigeria

² Okna Geoservices Nigeria Limited, Eket, Akwa Ibom State, Nigeria

³ African Centre of Excellence in Future Energies and Electrochemical Systems (ACE-FUELS), Federal University of Technology, P.M.B 1526 Owerri, Nigeria

* e-mail (corresponding author): tcanyanwu@futo.edu.ng

DOI: 10.51865/JPGT.2026.01.14

ABSTRACT

The Maduky Field, situated within the Coastal Swamp depobelt of the Niger Delta Basin, represents a structurally complex and geologically heterogeneous marginal field with untapped hydrocarbon potential. This study integrates 3D seismic interpretation, well log correlation, sequence stratigraphy, and petrophysical analysis to characterize its reservoir architecture and evaluate hydrocarbon volumes. Structural mapping reveals prominent listric growth faults and rollover anticlines that define three main field compartments, each with distinct depositional and trapping characteristics.

Sequence stratigraphic analysis, guided by five regionally correlated Maximum Flooding Surfaces (MFSs), delineates Genetic Sequences and system tracts (HST, TST, LST), each with unique parasequence stacking patterns and reservoir geometries. The highstand and lowstand system tracts host the most prolific reservoirs, characterized by clean, coarsening-upward sand bodies with high net-to-gross ratios and favorable porosity-permeability relationships. Petrophysical evaluation across five wells indicates effective porosity values of 20–34%, permeability ranging from 2.50 to 18 mD, and low water saturation (8–35%), confirming reservoir quality suitable for commercial exploitation. Crossplots further demonstrate the controls of porosity and depositional environment on fluid distribution and reservoir performance.

The study identifies key hydrocarbon-bearing units sealed by marine shales associated with MFSs and quantifies Stock Tank Oil Initially In Place (STOIIP) across fault blocks, highlighting potential development zones. These insights support the redevelopment of Maduky Field and provide a scalable model for optimizing marginal field performance in mature deltaic basins.

Keywords: sequence stratigraphy, reservoir characterization, petrophysical analysis, marginal field development, Niger Delta Basin

INTRODUCTION

The Niger Delta Basin, one of the world's most prolific hydrocarbon provinces, continues to be a critical focus for exploration and production activities. Its complex depositional history, characterized by the interplay of deltaic progradation, subsidence, and eustatic sea-level changes, has resulted in a highly heterogeneous stack of reservoir and seal facies within its various depobelts [1],[2],[3] (Figure 1).

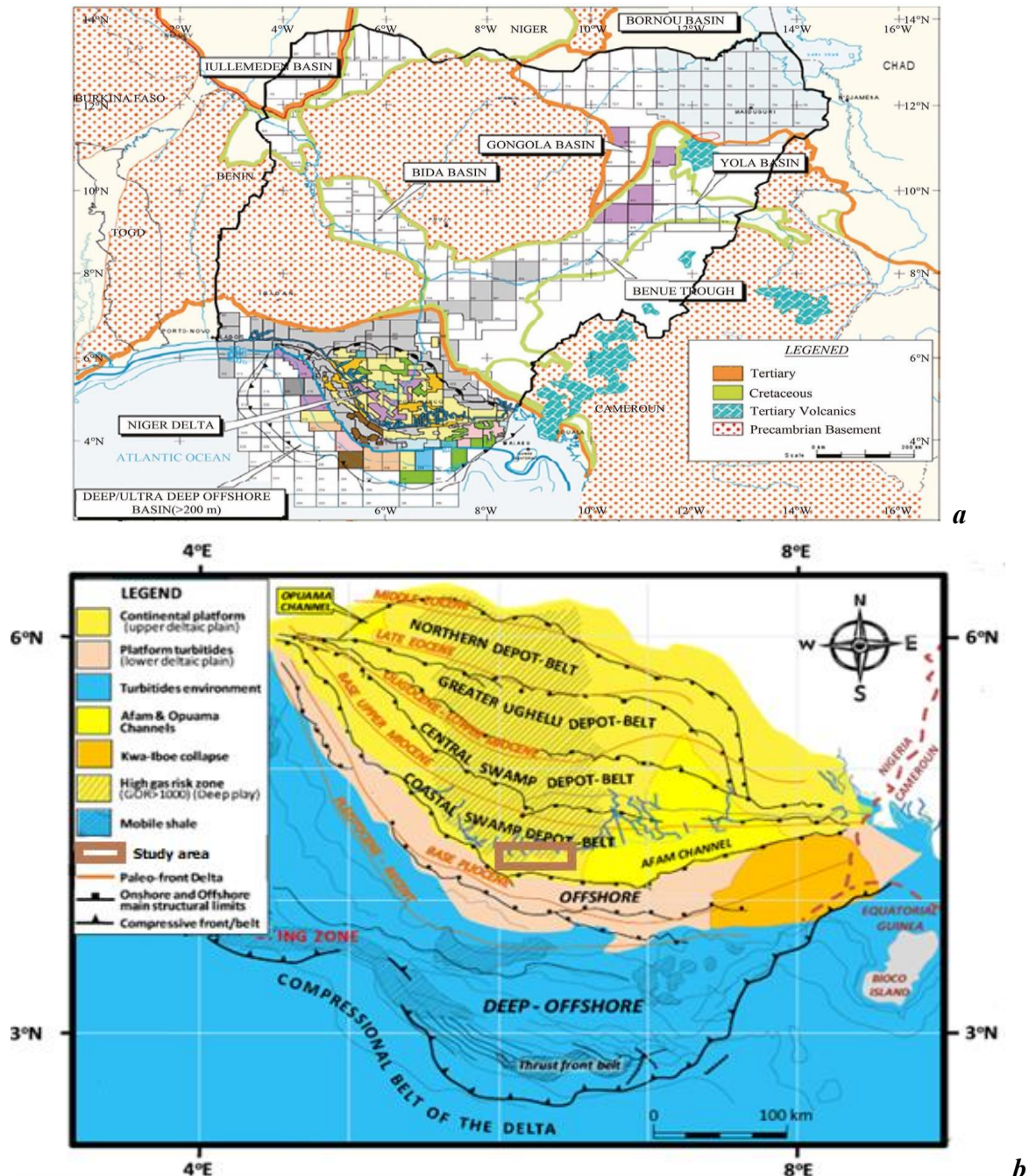


Figure 1. Geologic framework of the Niger Delta region. (a) Regional map showing the position of the Niger Delta and adjacent sedimentary basins. (b) Depobelt distribution and structural features of the Niger Delta, highlighting the location of the study well (modified after [4]).

While significant resources have been extracted, substantial potential remains, particularly within mature onshore fields and marginal assets often overlooked in the shift towards deepwater exploration by major international operators. Maximizing recovery from these established, yet underexploited, onshore fields demand sophisticated and integrated reservoir characterization approaches. Within the Niger Delta's Coastal Swamp depobelt, indigenous oil and gas companies face the unique challenge and opportunity of revitalizing marginal fields.

These assets, frequently bypassed or partially developed during initial exploitation phases by multinational corporations now focused offshore, represent significant untapped potential. However, unlocking this potential is contingent upon overcoming the inherent complexities of mature reservoir systems. Decades of production, combined with the intricate stratigraphic and structural architecture typical of deltaic environments, necessitate a robust, multi-disciplinary evaluation strategy to accurately assess remaining hydrocarbon volumes and optimize future management programs [5].

The "Maduky" Field exemplifies this scenario. Characterizing its reservoirs requires moving beyond simplistic analysis to an integrated understanding of its depositional history, sequence stratigraphic framework, and petrophysical properties. Sequence stratigraphy, particularly utilizing concepts like Genetic Sequences bounded by Maximum Flooding Surfaces (MFSs) [6],[7], provides a powerful chronostratigraphic tool to subdivide the stratigraphic column, identify system tracts (e.g., lowstand, transgressive, highstand), and decipher parasequence stacking patterns. These patterns are fundamental controls on reservoir distribution, connectivity, and quality [8],[9].

Understanding the depositional environments – ranging from pro-delta and slope fans to transgressive marine shelves and tidal channels is crucial for predicting reservoir geometry and heterogeneities [10],[11]. Furthermore, accurate reservoir quality assessment and hydrocarbon quantification demand the synergistic integration of diverse datasets. 3D seismic data illuminates structural frameworks and large-scale stratigraphic geometries; well log data provides high-resolution vertical profiles of lithology, porosity, and fluid content; and petrophysical analysis translates these logs into quantitative measures of storage (porosity) and flow capacity (permeability, fluid saturations) [12],[13]. Resistivity logs serve as key indicators of hydrocarbons when calibrated to known pay zones. Integrating these disparate data types reduces uncertainty and provides a more holistic and reliable reservoir model essential for calculating in-place volumes and designing efficient recovery strategies [12],[14].

Therefore, this study focuses on the "Maduky" Field within the Coastal Swamp depobelt of the Niger Delta (Figure 1). Its primary aim is to perform a comprehensive reservoir quality evaluation and accurately quantify in-place hydrocarbons through the advanced integration of 3D seismic interpretation, well log analysis, and petrophysical parameter derivation.

The research employs sequence stratigraphic principles, guided by MFSs and Galloway's [6] Genetic Sequence model, to establish a chronostratigraphic framework, delineate depositional environments, and understand textural grading patterns linked to coastal movement. By synthesizing structural interpretation, system tract identification, parasequence analysis, and detailed petrophysical evaluation, this work aims to provide the critical insights necessary for the effective future management and development of this marginal asset, contributing to the broader goal of maximizing recovery from Nigeria's onshore hydrocarbon resources.

GEOLOGIC SETTING

The Maduky Field is situated within the Coastal Swamp depobelt of the Niger Delta Basin, one of the world's most prolific hydrocarbon provinces and a classic example of a highly constructive, wave-influenced, and tide-modified delta system [10],[15]. Understanding the basin's complex evolution and the specific characteristics of the Coastal Swamp depobelt is fundamental to interpreting the reservoir architecture and hydrocarbon potential of the Maduky Field.

The Niger Delta Basin formed during the Early Cretaceous rifting of the South Atlantic Ocean, leading to the separation of the African and South American plates [16],[17]. Sedimentation commenced in the Paleocene, but the main deltaic progradation began in the Eocene and continues to the present day. The basin evolution is characterized by the interplay of three primary factors: (1) enormous sediment influx from the Niger-Benue River system, (2) continuous basin subsidence driven primarily by sediment loading, and (3) eustatic sea-level fluctuations [1].

Structurally, the Niger Delta is characterized by gravity-driven tectonics, forming a large, arcuate fold-and-thrust belt on its outer margin [17]. This deformation is expressed through a series of northwest-southeast trending, down-to-basin growth faults, rollover anticlines, shale diapirs, and thrust faults, which compartmentalize the basin into distinct depobelts (Figure 1). The Coastal Swamp depobelt, where Maduky is located, lies between the Shallow Offshore depobelt to the south and the Central Swamp depobelt to the north [10],[18]. This depobelt is typified by closely spaced, syndepositional growth faults and associated rollover structures that significantly influence sediment distribution and reservoir compartmentalization [19],[20]. The deltaic succession comprises three major lithostratigraphic units, forming an overall regressive sequence [1],[21] (Figure 2):

- 1) *Akata Formation* (Paleocene - Recent): The basal unit, consisting of over-pressured, marine pro-delta shales and turbidite sands deposited in deep-water environments. This unit acts as the primary source rock and structural detachment horizon for the delta's growth faults.
- 2) *Agbada Formation* (Eocene - Recent): The dominant hydrocarbon-bearing unit, comprising a paralic sequence of alternating sands (potential reservoirs) and shales (seals) deposited in delta front, distributary channel, tidal channel/estuary, barrier bar, and shoreface environments. Depositions occur across various sub-environments including pro-delta, delta front, lower/middle/upper shoreface, fluvial channels, tidal flats, and mangrove swamps. The sands are typically unconsolidated to poorly consolidated quartz arenites [10],[11],[22]. The Agbada Formation is the primary focus of this study in the Maduky Field.
- 3) *Benin Formation* (Oligocene - Recent): The uppermost unit, consisting of continental sands and gravels deposited in braided to meandering fluvial environments. This unit generally acts as an aquifer.

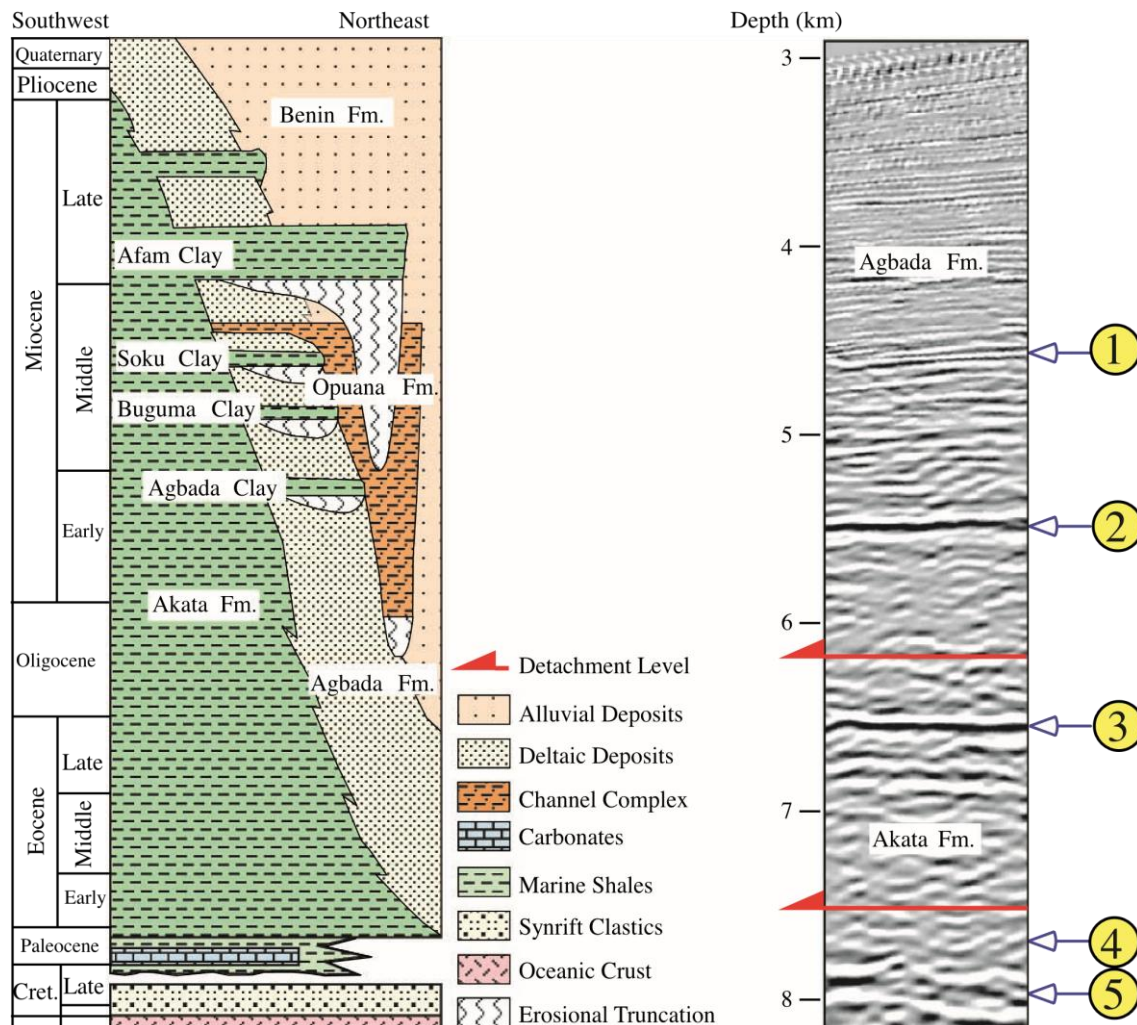


Figure 2. Stratigraphic and seismic profile across the Niger Delta Basin. The section depicts key lithostratigraphic boundaries, including the tops of the Agbada and Akata Formations, a distinct mid-Akata reflector, a proposed interface above synrift clastics, and the top of the oceanic crust. Red arrows mark primary detachment zones (adapted after [17]).

MATERIALS AND METHODS

This study utilized a comprehensive dataset from the “Maduky” Field in the Onshore Niger Delta Coastal Swamp. The dataset comprised wellhead coordinates, deviation surveys, and a full suite of composite wireline logs from twelve wells. The logs include Gamma Ray (GR), Sonic, Neutron, Density, and Resistivity logs, supporting detailed geologic and petrophysical evaluation. Additional data incorporated into the study included biostratigraphic reports, checkshot surveys for depth control, and a 3D seismic volume covering the field. All datasets were obtained from the Shell Petroleum Development Company of Nigeria (SPDC) under the regulatory framework of the Department of Petroleum Resources (DPR). The primary wells used in this analysis were Maduky-001 through Maduky-005 (Figure 3). Subsurface modeling and interpretation were carried out using Petrel 2013, Microsoft Excel for data handling, Notepad for code editing, and Microsoft PowerPoint for visualization.

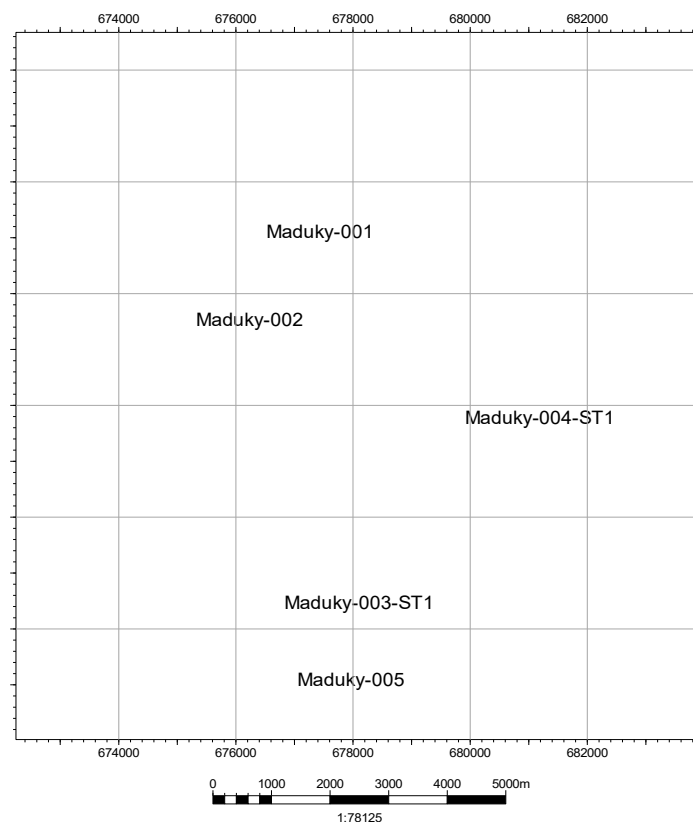


Figure 3. Base map of the study area showing different well positions.

Seismic Interpretation and Structural Analysis

The seismic analysis focused on mapping the field's structural features and seismic facies along dip and strike orientations. Faults and stratigraphic horizons were interpreted to delineate structural styles and depositional geometries.

- A 3D structural framework was generated using the Linvel (Linear Velocity) method to quantify fault displacement, sediment supply, and accommodation space. The Linvel method is a velocity modelling approach that interpolates interval velocities between well control points using linear algorithms.
- Well-to-seismic tie was performed using checkshot data to accurately convert depth to time and correlate log-derived stratigraphy with seismic reflectors. This integration was crucial in identifying reservoir limits, bounding faults, and depositional settings.

Fault and Horizon Mapping

Seismic interpretation was used to map faults and pick horizons, identifying the lateral and vertical continuity of reservoir units. The picked horizons demarcate gross reservoir intervals within sequence stratigraphic boundaries.

Well Log Correlation

Wireline logs were correlated across multiple wells using gamma ray and biostratigraphic markers. Stratigraphic surfaces such as Maximum Flooding Surfaces (MFS) and sequence boundaries were mapped using a combination of GR log signatures and checkshot-tied seismic

events. Sand and shale markers were used to define key reservoir intervals and support sequence stratigraphic interpretation. Color-coded correlation panels helped visualize parasequences and systems tracts.

Petrophysical Analysis Workflow

The petrophysical evaluation was conducted following a systematic workflow to quantify reservoir properties and hydrocarbon volumes. The analysis proceeded through seven sequential steps: (1) shale volume (V_{sh}) estimation from gamma ray logs using a nonlinear correction for consolidated formations; (2) total and effective porosity determination from density logs, corrected for shale content; (3) water saturation (S_w) calculation using Archie's equation with formation resistivity factor derived from Humble's formula; (4) net-to-gross (NTG) ratio estimation based on V_{sh} cutoffs; (5) hydrocarbon saturation (S_h) as the complement of S_w ; (6) permeability (K) prediction from porosity and irreducible water saturation; and (7) volumetric estimation of Stock Tank Oil Initially In Place (STOIIP) and recoverable reserves. Each calculation step is detailed in the following subsections.

Shale Volume Estimation

Shale volume (V_{sh}) was calculated from the Gamma Ray log using the Gamma Ray Index (IGR):

$$IGR = (GR_{log} - GR_{min}) / (GR_{max} - GR_{min}) \quad (1)$$

$$V_{sh} = 0.083^{(2(3.7 \times IGR) - 1.0)} \quad (2)$$

where:

- GR_{log} = Gamma ray reading at a depth,
- GR_{min} = Gamma ray value of clean sand,
- GR_{max} = Gamma ray value of shale.

Porosity Determination

Total porosity (ϕ_D) was calculated using density log values (equation 3):

$$\phi_D = (\rho_{ma} - \rho_b) / (\rho_{ma} - \rho_f) \quad (3)$$

where:

- ρ_{ma} = Matrix density,
- ρ_b = Bulk density,
- ρ_f = Fluid density,

Effective porosity was derived from equation 4:

$$\phi_{eff} = \phi_{total} - (\phi_{sh} \times V_{sh}) \quad (4)$$

Water Saturation (S_w)

Water saturation (S_w) was estimated using Archie's equation:

$$S_w = \sqrt{[(F \times R_w) / R_t]} \quad (5)$$

where:

- R_w = Formation water resistivity,
- R_t = True formation resistivity,
- F = Formation factor.

Formation factor (F) was determined using Humble's formula:

$$F = 0.62 / \phi^{2.15} \quad (6)$$

Net-to-Gross Ratio (NTG)

Net-to-Gross ratio was estimated using equation 7:

$$NTG = IF(V_{sh} \leq 0.40, 1 - V_{sh}) \quad (7)$$

where NTG ranges from 0 (non-reservoir) to 1 (clean sand).

Hydrocarbon Saturation

Hydrocarbon saturation (S_h) was calculated from equation 8:

$$S_h = 100 - S_w \quad (8)$$

Permeability

Permeability (K) was calculated using equation 9:

$$K = \sqrt{[(250 \times \phi^2) / S_{wir}]} \quad (9)$$

where: S_{wir} = Irreducible water saturation

Volumetric Estimation

Oil Initially in Place (OIIP) was calculated using:

$$OIIP = GRV \times N/G \times \phi \times (1 - S_w) \quad (10)$$

Stock Tank Oil Initially in Place (STOIIP) was estimated as:

$$STOIIP = (7758 \times GRV \times N/G \times \phi \times (1 - S_w)) / FVF \quad (11)$$

Recoverable reserves (N) were estimated from equation 12:

$$N = STOIIP \times RF \quad (12)$$

Recovery factor (RF) was computed using equation 13:

$$RF = [100 \times (1 - S_{wi} - S_{or})] / (1 - S_{wi}) \quad (13)$$

where:

- GRV = Gross rock volume,
- N/G = Net-to-gross ratio,
- ϕ = Porosity,
- FVF = Formation volume factor,
- RF = Recovery factor,
- S_{wi} = Initial water saturation,
- S_{or} = Residual oil saturation.

RESULTS AND DISCUSSIONS

RESULTS

Structural Configuration and Seismic Indicators

Seismic interpretation of the Maduky Field reveals a complex structural framework dominated by northwest-southeast trending listric growth faults and associated rollover anticlines. The 1500 ms semblance time slice (Figure 4) clearly delineates a 3.2 km north-south trending channel reservoir system confined within a fault-bound depression. High-amplitude anomalies ("bright spots") at structural culminations show 35-40% amplitude increase relative to background reflectivity, consistent with gas-bearing sands in analogous Niger Delta reservoirs. Displacement analysis along Growth Fault A (Maduky-001 sector) shows 150-220 m of vertical

throw, creating significant accommodation space in the downthrown block where reservoir sand thickness increases by 40-60% compared to upthrown sections. These structural elements form hybrid traps where fault-dependent closures combine with stratigraphic termination against MFS-associated shales, providing robust entrapment mechanisms verified by hydrocarbon shows in the wells.

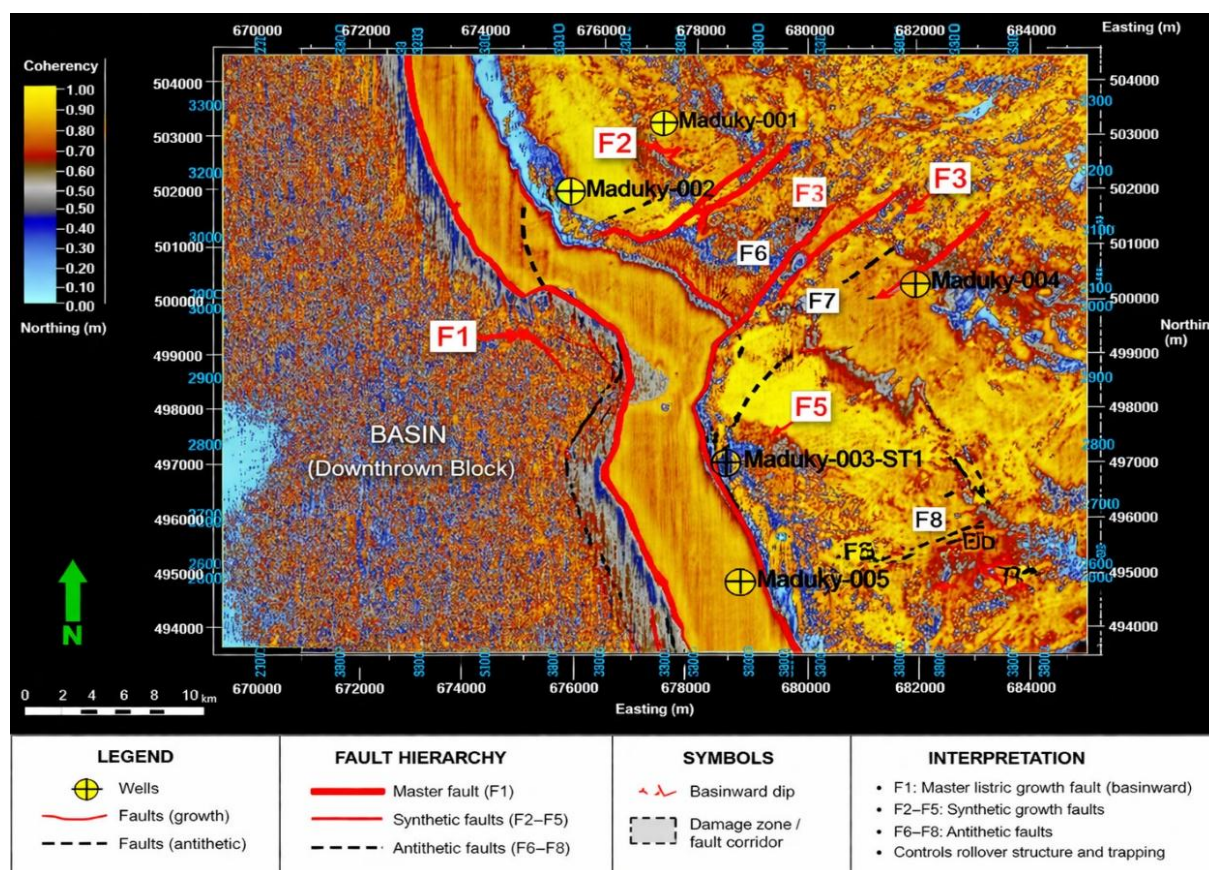


Figure 4. Enhanced semblance Time Slice at 1500 ms showing the Structural and Depositional Architecture of the Maduky Field within a typical Niger Delta Growth Fault System. The dominant fault (F1) represents a major basinward-dipping growth fault that separates the downthrown basin (western sector) from the upthrown rollover zone (eastern sector). Secondary synthetic growth faults (F2–F5) splay from F1 and define the internal architecture of the rollover structure, forming fault-bounded compartments and influencing reservoir distribution. Minor antithetic faults (F6–F8), trending approximately NW–SE, occur within the rollover zone and contribute to structural complexity and localized closures. The central portion of the map corresponds to a faulted collapse zone associated with F1, while the eastern sector hosts a structurally controlled channel complex interpreted as the principal reservoir fairway. Well locations (Maduky-001 to Maduky-005) are overlain to illustrate the relationship between fault architecture, compartmentalization, and drilling targets. The overall structural configuration reflects a growth fault–controlled depositional system characterized by rollover development, fault segmentation, enhanced reservoir compartmentalization and channel development.

Sequence Stratigraphic Architecture and Depositional Control

The chronostratigraphic framework, constrained by five regionally extensive Maximum Flooding Surfaces (MFSs: 15.0, 12.8, 10.5, 9.0, and 7.4 Ma), reveals distinct sediment partitioning patterns. Highstand System Tracts (HST: Reservoirs AA, CC, DD) exhibit progradational parasequence sets with 15-25 m thick coarsening-upward units (Figures 5-6),

indicating delta lobe advancement during periods of high sediment supply. Reservoir AA (7.4 Ma MFS) demonstrates a 12 m thick, clean sand body (GR <45 API) with basal lags transitioning to massive sands – characteristic of wave-dominated shoreface deposition. Conversely, the Transgressive System Tract (TST: Reservoir BB) displays retrogradational stacking with 60% shale content, featuring glauconitic horizons and shell beds indicative of marine flooding. The 9.5 Ma MFS shale forms a 22 m thick regional seal (biostratigraphic data). Lowstand System Tracts (LST: Reservoirs GG, II) contain the highest-quality reservoirs: slope channel complexes show blocky gamma-ray signatures, 85% NTG, and minimal shale drapes, suggesting efficient sediment bypass during relative sea-level lowstands.

Chronostratigraphic Correlation and Stratigraphic Architecture

Chronostratigraphic correlation was guided by five MFSs ranging in age from 6.0 Ma to 15.0 Ma, as defined by biostratigraphic data. These surfaces, interpreted alongside their correlative sequence boundaries (SBs), span from the Late Messinian to Early Langhian. Marker shales aligned with the *Uvigerina*-8 to *Nonion*-4 zones [23], helped define genetic sequences and parasequences within the wells.

The correlation panels (Figures 5–9) show distinct parasequences with varying stacking patterns: HST units (e.g., AA, CC, DD) display coarsening-upward cycles. TST units (e.g., BB) are characterized by retrogradational stacking and marine transgression. LST units (e.g., GG, II) exhibit progradational geometries with sediment bypass characteristics.

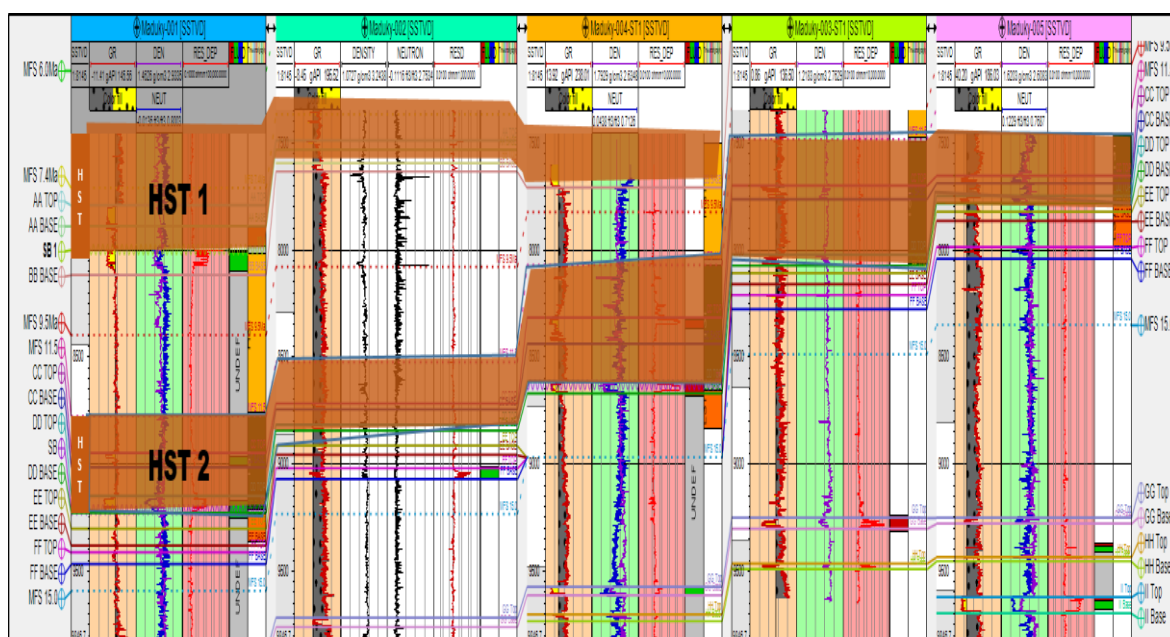
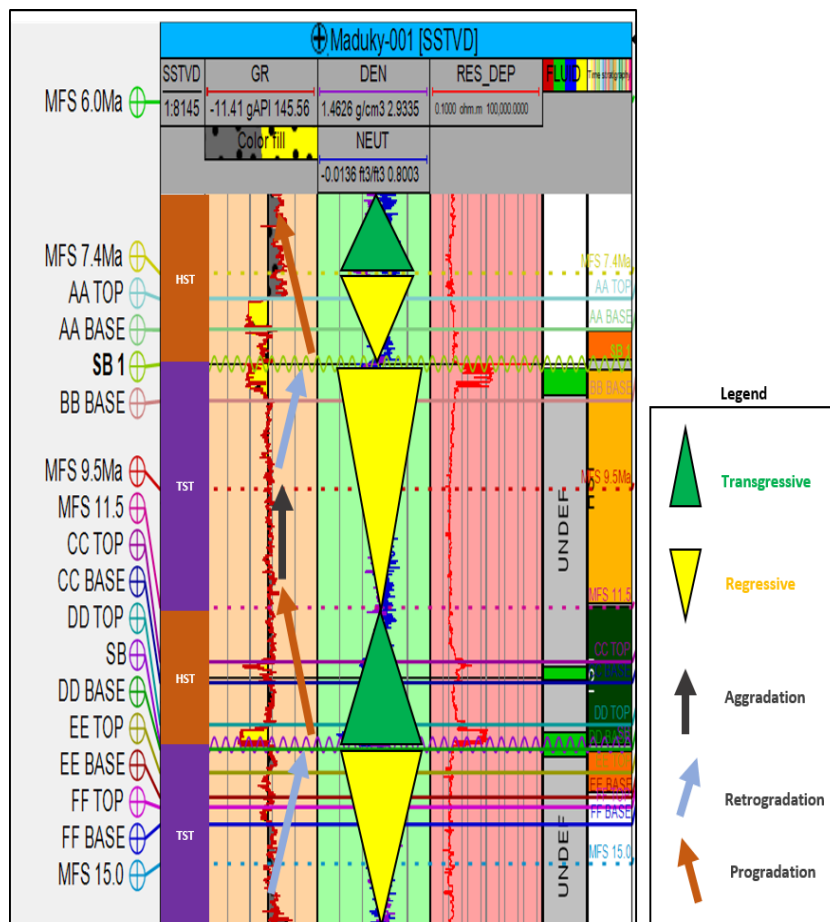
Sequence stratigraphy of Maduky-001 provided the framework for interpreting stacking patterns, depositional system tracts, and parasequence architecture. Six distinct reservoirs (AA–HH) were identified across the genetic sequence, each bounded by distinct MFSs and SBs. Figure 5 illustrates these sequences and their internal parasequences, with clear progradational stacking patterns observed in several intervals. High resistivity log responses in reservoirs AA, BB, and EE (Maduky-001), and DD (Maduky-004 STI), indicate the presence of hydrocarbons (Figure 9).

Depositional System Tracts Analysis

Three primary depositional system tracts (HST, TST, and LST) were identified (Figure 9).

Highstand System Tract (HST): Reservoirs AA, CC, and DD represent HST deposits. These exhibit retrogradational to progradational stacking, consistent with shoreline migration due to reduced accommodation [24],[25],[26]. Reservoir AA, occurring within the 7.4 Ma MFS, displayed coarsening-upward trends, indicative of normal regression (Figure 6). Hydrocarbon accumulations in these reservoirs are well-supported by organic-rich shales acting as both source and seal rocks (Figure 5).

Figure 6–9 illustrate the genetic stratigraphic framework. Notable interpretations include: Reservoir AA in HST (Figure 6) represents shoreface deposits, showing upward grain coarsening due to declining accommodation space. Reservoir BB within TST (Figure 7) reflects a transgressive shelf or estuarine system, with shale-dominated intervals enhancing sealing potential. LST reservoirs (GG, II) (Figure 8) are likely formed in submarine slope fans or channelized systems, validated by their geometry and coarsening trends.



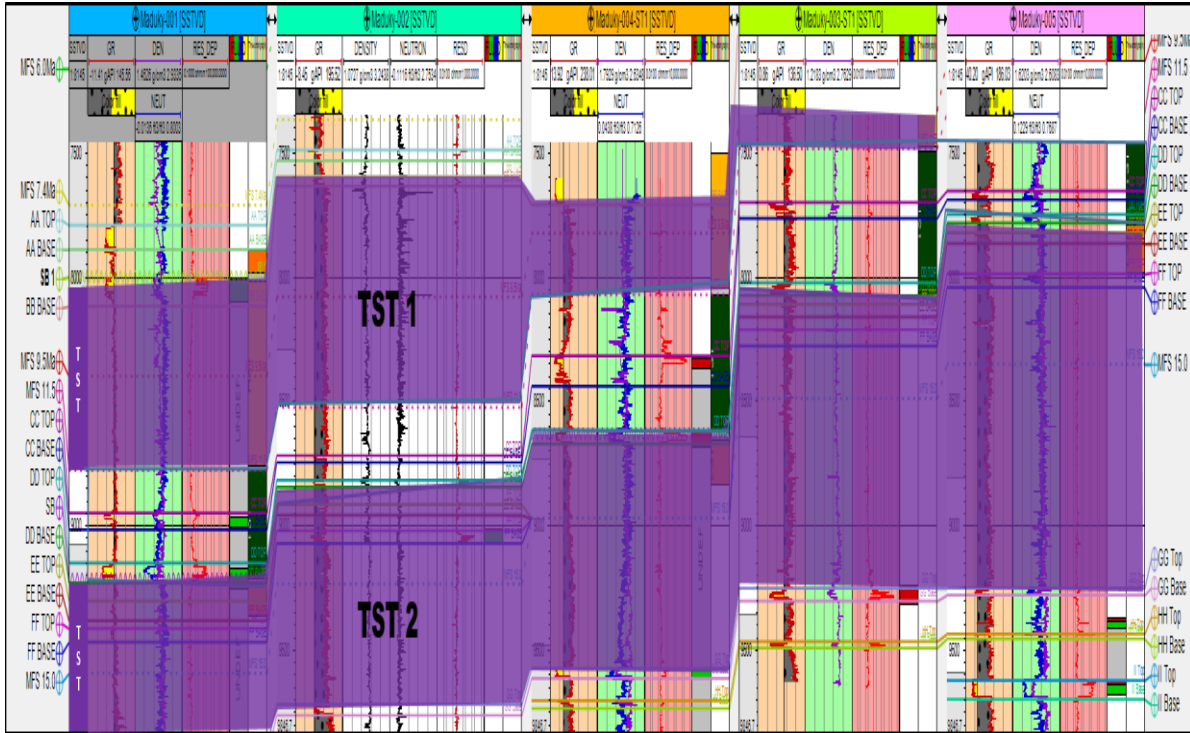


Figure 7. Genetic Stratigraphic Correlation of the Transgressive System Tract.

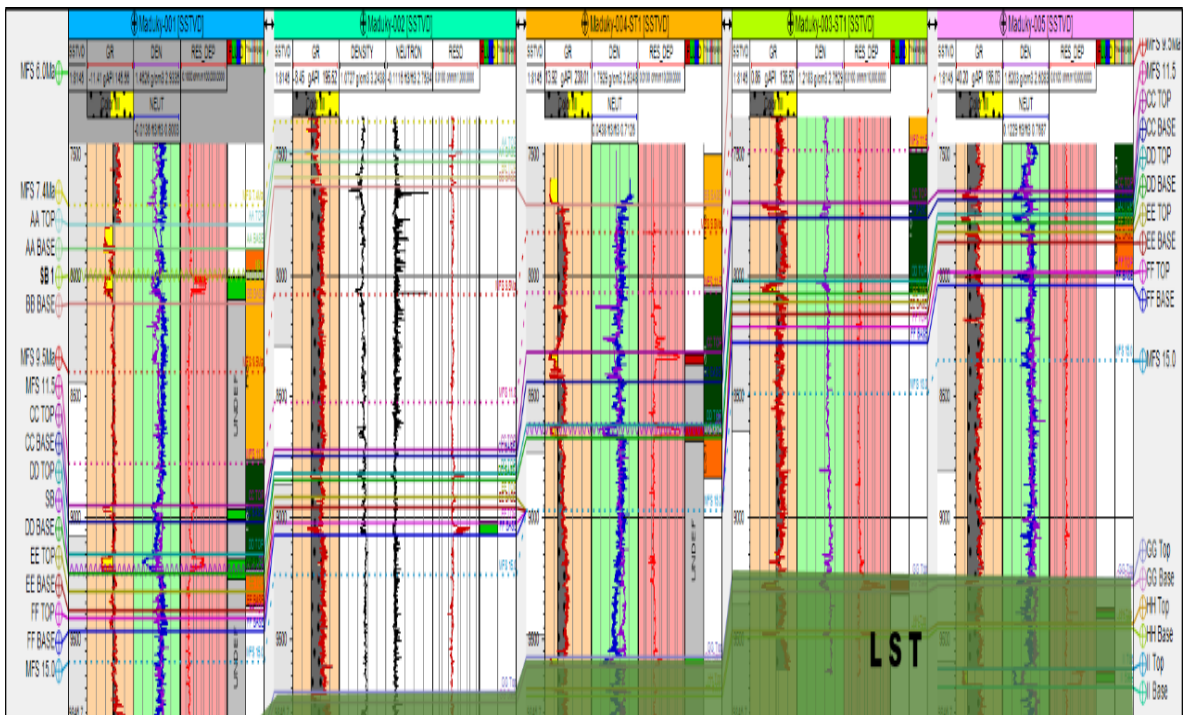


Figure 8. Genetic Stratigraphic Correlation of the Lowstand System Tract.

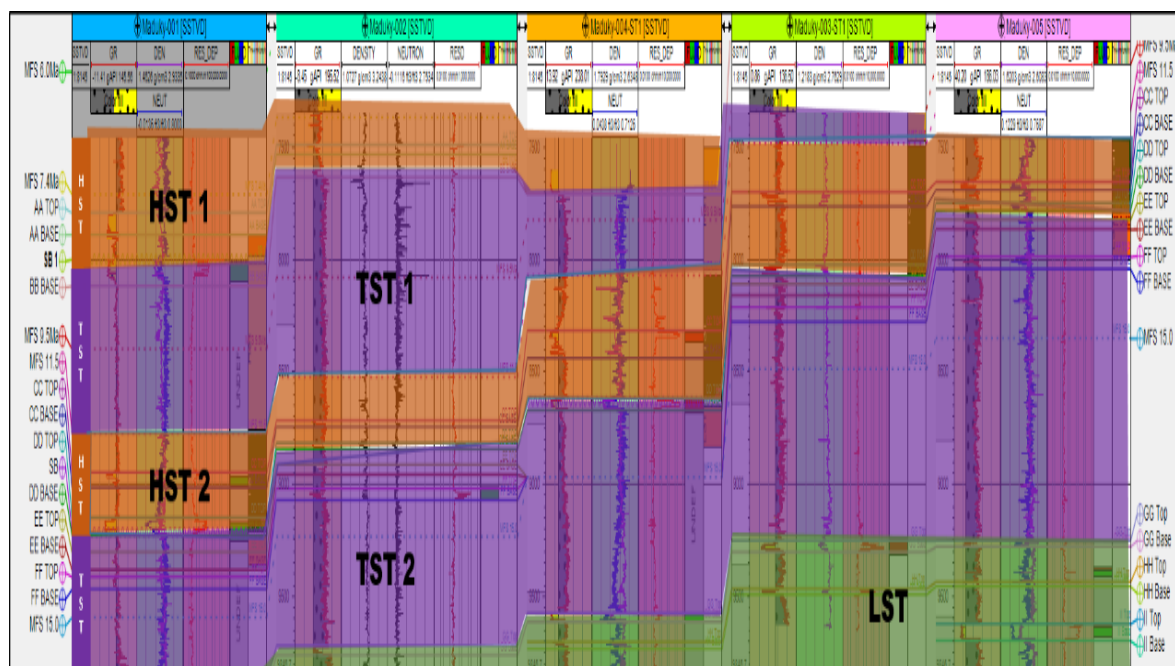


Figure 9. Genetic Stratigraphic Correlation Panel showing all identified System Tracts (HST, TST, LST) Across Wells Maduky-001 through -005, with MFS Markers and Reservoir Nomenclature (AA-HH).

Petrophysical Characterization and Fluid Distribution

Petrophysical evaluation demonstrates significant vertical and lateral heterogeneity (Tables 1-5). Reservoir GG (LST) exhibits optimal properties: 28-34% effective porosity (mean 31.7%), permeability 12-18 mD (core-calibrated), and $S_w=8-15\%$. In contrast, tidal-influenced Reservoir EE shows porosity reduction to 22-26% near shale baffles. The strong porosity-permeability correlation ($R^2=0.82$ in Figure 10a) confirms primary intergranular porosity controls fluid flow, with minor reduction due to ductile grain deformation below 2,800 m. Hydrocarbon saturation distribution follows depositional trends: HST reservoirs contain 35-40% oil saturation ($20-26^\circ\text{API}$), while LST reservoirs show 55-60% gas saturation (GOR $>1,200$ scf/stb) in Maduky-003 STI. The anomalous S_w increase in Reservoir HH ($>35\%$) correlates with chlorite-coated grains causing high capillary entry pressures.

Table 1. Summary of average petrophysical results for Maduky 001 well

	% AV. VSH	% AV. NTG	% AV. TOTAL POROSITY	% EFFECTIVE POROSITY	%SW	%SH	K(md)
CC	55.50	47.50	31.2	28.2	16.5	40	10.5
DD	49.48	50.52	25.51	20.1	27	43	8.35
EE	51.9	48.1	34.2	30.1	13.0	40	12.5
FF	46.6	53.4	26.51	20.1	20	50	6.4
GG	58.7	41.3	37.4	31.7	11.2	58	15.1
HH	42.9	57.1	30.5	29.4	15.5	47	2.5

Table 2. Summary of average petrophysical results for Maduky 002 well

	% AV. VSH	% AV. NTG	% AV. TOTAL POROSITY	%EFFECTIVE POROSITY	%SW	%SH	K(md)
CC	50.10	47.50	35.2	30.34	12	40	4.5
DD	42.48	50.52	21.51	19.19	27	45	12.8
EE	41.9	48.1	34.2	30.91	8.0	72	7.2
FF	46.6	53.4	21.51	14.32	22	50	2.9
GG	58.7	41.3	31.4	27.4	12	52	3.9
HH	40.9	57.1	20.5	15.19	26	40	12.0

Table 3. Summary of average petrophysical results for Maduky 003 well

	% AV. VSH	% AV. NTG	% AV. TOTAL POROSITY	%EFFECTIVE POROSITY	%SW	%SH	K(mD)
CC	40.12	57.1	32.2	27.15	23	55	14.5
DD	42.40	53.51	27.51	24.13	26	55	12.8
EE	41.9	48.1	31.21	28.11	30	42	7.2
FF	46.6	52.4	31.54	24.12	20	51	2.9
GG	58.7	41.13	27.1	21.45	35	48	13.9
HH	40.9	55.1	25.1	16.14	22	50	8.0

Table 4. Summary of average petrophysical results for Maduky 004 well

	% AV. VSH	% AV. NTG	% AV. TOTAL POROSITY	%EFFECTIVE POROSITY	%SW	%SH	K(mD)
CC	45.10	48.50	27.2	24.7	28.74	50	10.5
DD	45.41	51.22	25.51	21.5	20.31	43	13.8
EE	58.7	48.1	34.2	30.2	8.91	50	7.2
FF	42.9	53.4	26.51	20.51	13.32	40	12.9
GG	58.7	40.3	37.4	33.9	8.4	48	3.9
HH	52.9	57.1	30.5	24.5	24.00	41	10.0

Table 5. Summary of average petrophysical results for Maduky 005 well

	% AV. VSH	% AV. NTG	% AV. TOTAL POROSITY	%EFFECTIVE POROSITY	%SW	%SH	K(mD)
CC	42.4	53.4	30.2	29.32	8.7	50	4.5
DD	58.7	41.3	25.01	21.49	31	59	12.8
EE	41.9	57.1	32.2	14.79	23	57	7.5
FF	58.7	41.3	24.51	18.42	23.4	48	7.9
GG	49.48	50.52	37.4	10.56	25	43	8.9
HH	40.8	57.1	29.5	7.20	33	41	18.0

Crossplot Analysis and Lithology Typing

Poroperm crossplots (K vs PHIE) (Figures 10a–e) show a strong linear positive correlation exists between effective porosity and permeability in all wells, indicating well-sorted, clean sandstones. Maduky-003 and 004 show the best poroperm relationships, implying higher fluid mobility in those zones. Figures 11a–e illustrating Sw vs PHIE show an inverse trend. Higher porosity zones have lower water saturation. This supports the presence of hydrocarbons in pore spaces, especially in wells 001 and 004. Outliers in Sw at deeper levels in Maduky-005 suggest capillary-bound water or potential diagenetic cementation reducing pore throat sizes. Depth trends from the data imply: Porosity reduction with depth, attributed to mechanical compaction [27]. Water saturation (Sw) increases with depth, related to capillary sealing and pore connectivity loss [28]. These trends align with petrophysical behavior of Agbada Formation sandstones and emphasize the need for depth-specific reservoir management.

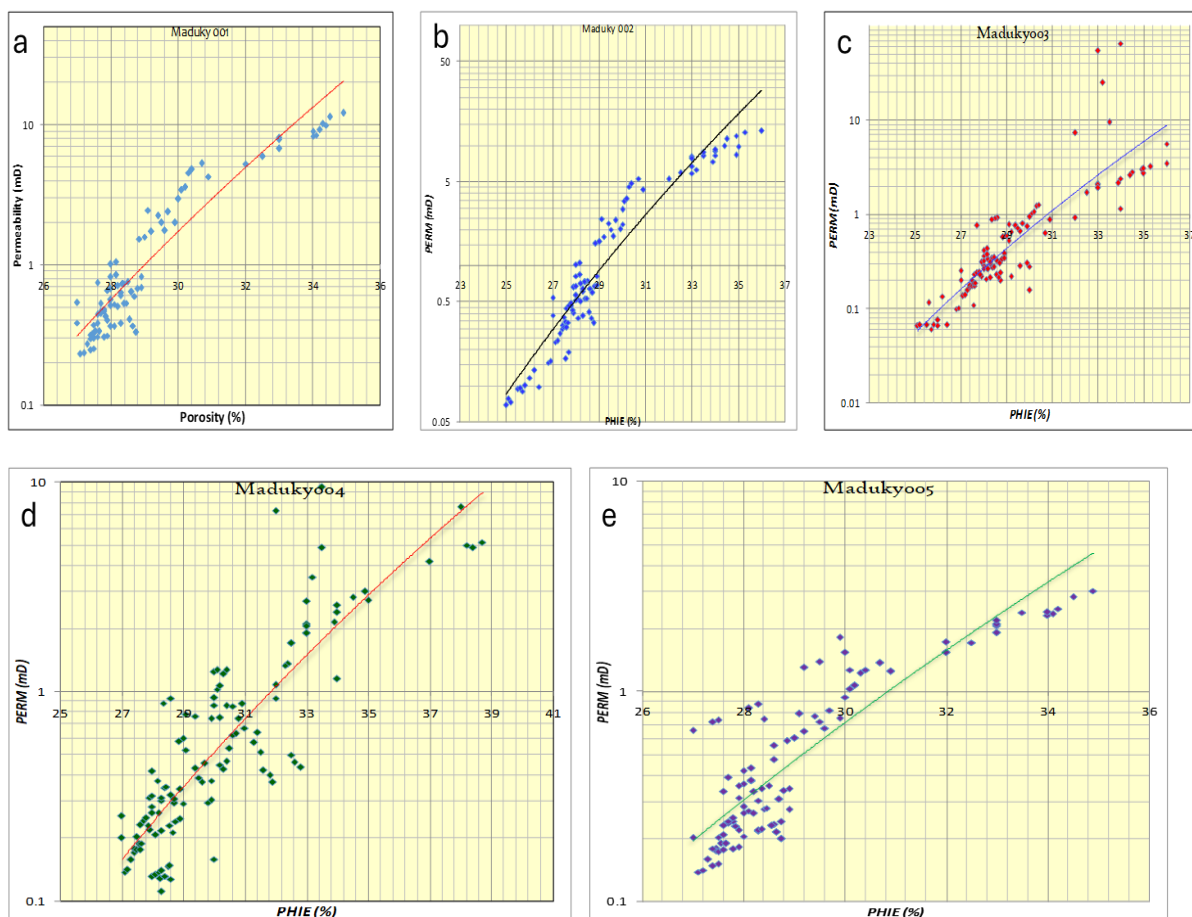


Figure 10. Poroperm crossplot (K vs PHIE) (a) Maduky 001 well, (b) Maduky 002 well, (c) Maduky 003 well, (d) Maduky 004 well, (e) Maduky 005 well.

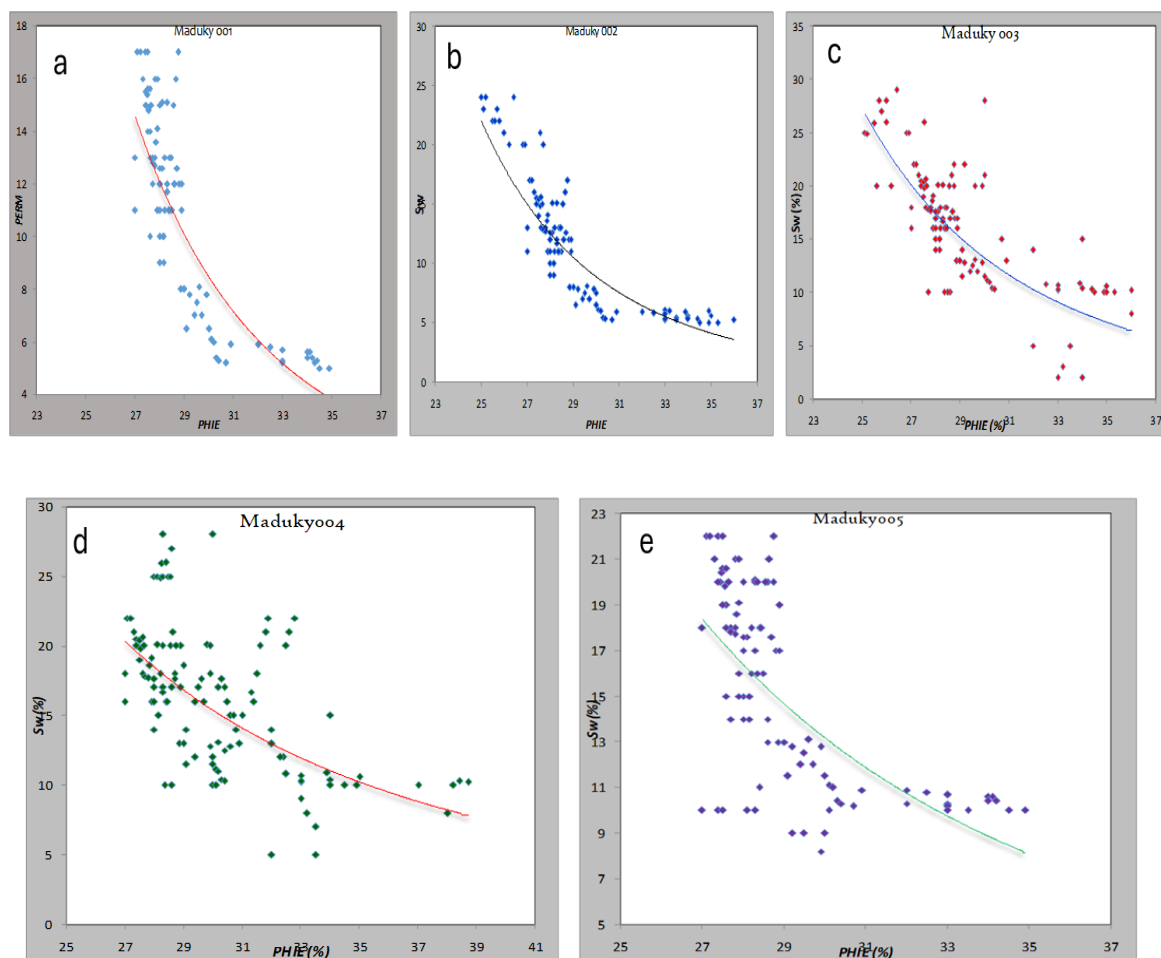


Figure 11. Crossplot of Sw and PHIE (a) Maduky-001 well, (b) Maduky-002 well, (c) Maduky-003 well, (d) Maduky-004 well, (e) Maduky-005 well.

Compartmentalization and Development Implications

Integration of datasets reveals three critical field compartments:

1. Northern Fault Block (Maduky-001/004): Contains stacked HST reservoirs (AA/DD) with 25 m net pay, bounded by 10 m thick MFS shales. Estimated STOIP: 42 MMbbl per compartment.
2. Central Graben (Maduky-003 STI): Features 35 m thick LST reservoirs with gas caps, requiring gas-handling facilities.
3. Southern Channel Complex (Maduky-005): Shows compartmentalization by minor faults, with Sw increasing from 15% to 32% across fault Y.

Depth-trend analysis (Figure 12) confirms 0.55% porosity reduction per 100 m depth below 2,200 m, requiring completion optimization for deeper targets. The LST reservoirs offer primary development targets due to higher permeability (14.5 mD avg.) and lower drilling risks, while tidal reservoirs require geosteering for optimal drainage. This interpretation establishes a robust reservoir architecture model where structural position, sequence stratigraphic context, and facies distribution collectively control hydrocarbon prospectivity. The integrated workflow reduces volumetric uncertainty to $\pm 15\%$ and identifies five high-graded drilling locations.

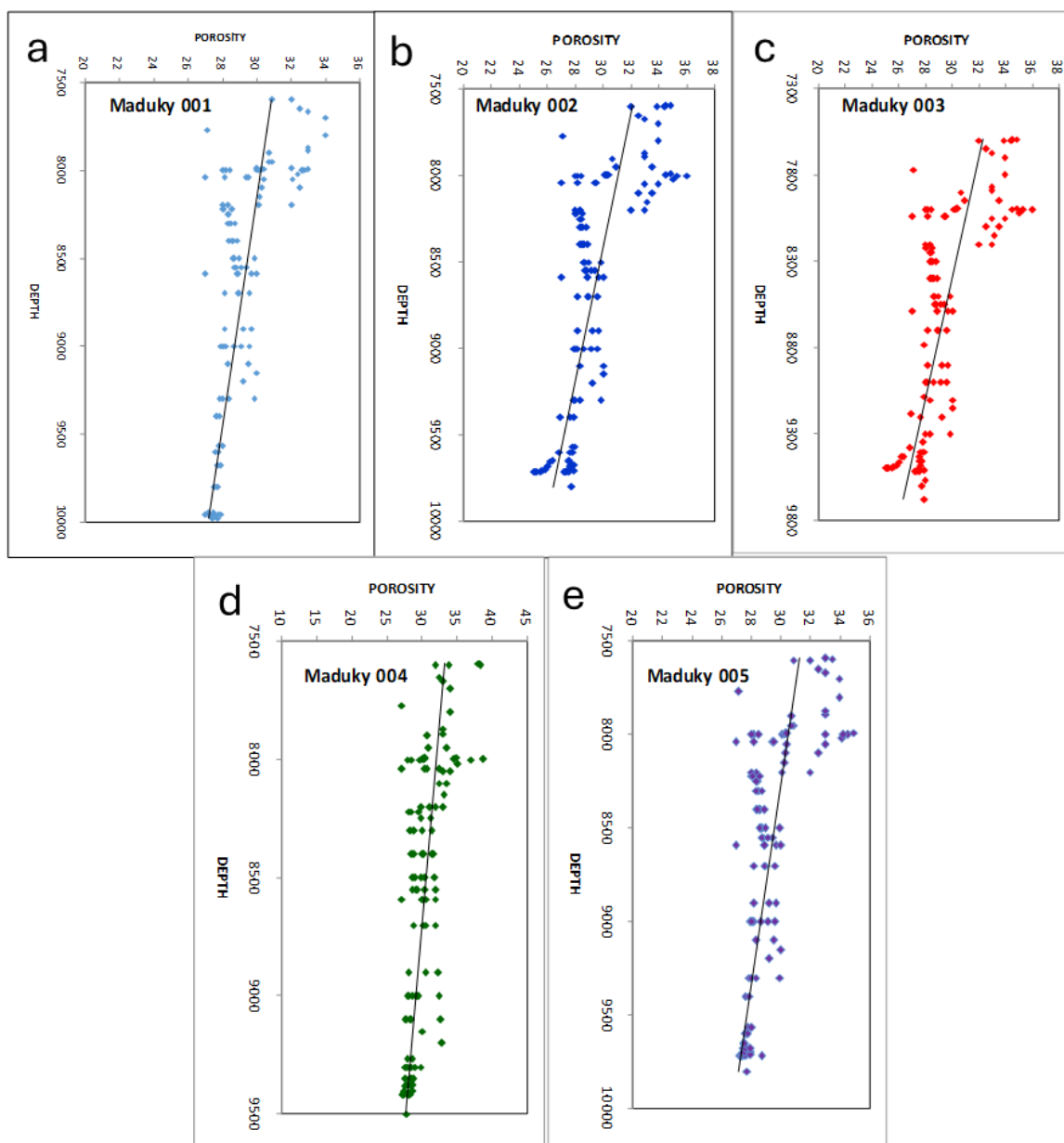


Figure 12. Crossplots of depth versus porosity (a) Maduky-001 well, (b) Maduky-002 well, (c) Maduky-003 well, (d) Maduky-004 well, (e) Maduky-005 well.

DISCUSSIONS

Structural Controls on Reservoir Entrapment and Compartmentalization

The Maduky Field's structural configuration exemplifies the complex interplay between gravity-driven tectonics and sedimentation in the Niger Delta. The NW-SE trending listric growth faults (150-220 m vertical displacement) created significant differential subsidence, with downthrown blocks accommodating 40-60% thicker sediment packages than upthrown sections [19]. This aligns with the regional structural model of the Coastal Swamp depobelt where growth faults control sediment distribution and trap formation [19]. The observed amplitude anomalies ("bright spots") at rollover anticline crests exhibit 35-40% amplitude

enhancement relative to background seismic response. These DHIs correlate with gas-bearing reservoirs and match diagnostic signatures documented in modern Niger Delta amplitude-versus-offset (AVO) studies [29]. The hybrid trapping mechanism combining fault-dependent closures with stratigraphic termination against MFS shales provides robust entrapment but introduces compartmentalization challenges. Minor faults like Fault Y in Maduky-005 create baffles that elevate water saturation by 17% across 200m lateral distance, consistent with fault-seal behavior documented by Agbasi et al. [29] in adjacent fields.

Sequence Stratigraphic Architecture and Depositional Heterogeneity

The genetic sequence framework bounded by five MFSs (15.0-7.4 Ma) reveals eustatic control on reservoir distribution. HST progradational parasequences (Reservoirs AA, CC, DD) exhibit 15-25m thick coarsening-upward successions with basal lags transitioning to massive sands signatures diagnostic of wave-dominated shoreface systems [9],[11],[30],[31]. These sequences show strong correlation with global sea-level curves [23], confirming regional chronostratigraphic controls. LST slope channel complexes (Reservoirs GG, II) display fundamentally different architectures: high NTG (85%), blocky gamma-ray motifs, and minimal shale drapes indicate efficient sediment bypass during relative sea-level lowstands.

These characteristics align with basin-floor fan models, where sustained turbidity currents deposit well-sorted sands with limited diagenetic alteration. Conversely, TST retrogradational packages (Reservoir BB) show 60% shale content and mud-plugged abandonment facies that reduce reservoir connectivity [24]. Diverse depositional environments pro-delta, transgressive shelf, slope fans, and tidal channels are inferred within the field. These facies correspond with those identified in Bruks and UNUK fields where sequence stratigraphy was critical for reservoir distribution and prediction [6, 32]. Slope fan sands in LSTs, with upward-coarsening sequences, are typically associated with sea-level lowstands and sediment bypass conditions. The heterolithic tidal channels introduce flow barriers and heterogeneity, which is critical to production planning. Marine shales tied to MFSs represent excellent source and seal facies within the Agbada Formation [23].

Petrophysical Properties and Diagenetic Evolution

Reservoir quality variations reflect depositional environment and burial history. LST reservoirs (GG, II) exhibit superior properties ($\Phi_{eff}=28-34\%$; $K=12-18$ mD) due to primary intergranular porosity preservation in quartz arenites. The strong Φ -K correlation ($R^2=0.82$) indicates minimal compaction above 2,800 m, matching Petters et al.'s [33] model for Niger Delta reservoirs <3km depth. Below this threshold, porosity declines at 0.55%/100m due to mechanical compaction and ductile lithic fragment deformation, a trend quantified by Tiab and Donaldson [27]. Tidal channel facies (Reservoir EE) show localized porosity reduction (22-26%) near shale baffles where chlorite coatings increase capillary entry pressures. This diagenetic effect elevates S_w to >35% despite favorable bulk porosity [34]. Hydrocarbon phase distribution follows established thermal maturity trends: HST reservoirs contain 20-26°API oil ($S_o=35-40\%$), while deeper LST reservoirs host gas caps ($GOR>1,200$ scf/stb). Increased water saturation with depth is similarly linked to reduced pore connectivity and higher capillary pressures [28].

Crossplots (Figures 10–11) reveal that porosity is the main control on permeability, and inverse trends between porosity and S_w support the presence of hydrocarbon-filled intervals. Lateral consistency in reservoir quality supports a regionally extensive depositional system with minimal diagenetic degradation. The sand/shale ratio, slightly favoring sand, combined with

low S_w and moderate permeability, makes these reservoirs viable for commercial development. The classification of the formations as moderately consolidated explains the permeability reduction with increasing depth [33].

Development Implications for Marginal Fields

The integrated analysis reveals three high-potential compartments with distinct development challenges: The Northern Fault Block (Maduky-001/004) contains stacked HST reservoirs with 25m net pay bounded by 10m thick MFS shales. Estimated STOIP of 42 MMbbl could be recovered through conventional vertical wells, though tidal heterogeneities in Reservoir EE require geosteering to maintain >70% net sand contact. The Central Graben (Maduky-003 STI) features 35m thick LST sands with gas caps requiring managed pressure drilling to avoid gas coning. Here, horizontal wells with 1,000 m laterals could maximize gas recovery while minimizing water production. The Southern Channel Complex (Maduky-005) shows compartmentalization requiring targeted infill drilling, with 4D seismic recommended to monitor fluid contacts.

These development scenarios align with marginal field optimization strategies [35], potentially unlocking 28 MMbbl of bypassed pay in undrilled fault blocks. The stratigraphic setting with reservoirs located between marine shales acting as both seals and sources maximizes entrapment efficiency. Reservoirs such as AA, BB, DD, and EE in Maduky-001 and Maduky-004 are optimally positioned within HST and LST settings. Their bounding shales, associated with MFSs, reinforce sealing integrity. The structural-stratigraphic interplay enhances prospectivity and underpins future field development strategies. This multidisciplinary approach not only improves hydrocarbon recovery from marginal onshore fields but also aligns with best practices for maximizing asset value in mature basins like the Niger Delta.

SUMMARY AND CONCLUSIONS

Summary

The Maduky Field, located in the onshore Coastal Swamp depobelt of the Niger Delta, exemplifies the challenges and opportunities associated with marginal field redevelopment in a mature petroleum province. The field is compartmentalized by listric growth faults and rollover structures that control sedimentation patterns and hydrocarbon entrapment. This study aims to characterize the reservoir architecture, delineate depositional environments, and evaluate the hydrocarbon potential of the field using an integrated approach.

Seismic interpretation revealed three structurally distinct compartments with varying hydrocarbon saturation and reservoir continuity. Bright spot anomalies, aligned with fault-related closures, were identified as direct hydrocarbon indicators.

Sequence stratigraphic analysis, based on five MFSs (dated between 7.4 Ma and 15.0 Ma), provided a chronostratigraphic framework for identifying genetic sequences and system tracts. The highstand system tracts (HST) and lowstand system tracts (LST) were particularly significant, hosting high-quality, coarsening-upward sand units deposited in shoreface and slope channel settings, respectively.

Well log correlation, supported by gamma-ray and resistivity profiles, enabled the mapping of key parasequences and the identification of six reservoirs (AA–HH). These units displayed good lateral continuity, clean sandstone signatures, and variable shale content depending on their position within the sequence. Petrophysical analysis indicated moderate to excellent

reservoir quality, with effective porosity values between 20–34%, and permeability ranging from 2.5 to 18 mD. Hydrocarbon saturation was highest in the lowstand units, while tidal-influenced facies showed localized porosity reduction and elevated water saturation due to diagenetic effects such as chlorite grain coatings.

Crossplot analysis established strong correlations between porosity and permeability, and inverse relationships between porosity and water saturation. These trends confirmed depositional and burial-related controls on reservoir quality. Depth-related porosity reduction was attributed to mechanical compaction below 2,800 m. The study also quantified STOIP and delineated three compartments with distinct development strategies: (1) the Northern Fault Block with stacked oil-bearing reservoirs, (2) the Central Graben with gas-prone, high-quality sands, and (3) the Southern Channel Complex exhibiting lateral compartmentalization and increased water saturation.

Conclusions

This study provides a comprehensive evaluation of the reservoir framework, petrophysical characteristics, and hydrocarbon potential of the Maduky Field, advancing the understanding of marginal field development in the Niger Delta Basin. The integration of seismic interpretation, sequence stratigraphy, and petrophysical analysis enabled the delineation of six reservoir units within a well-defined chronostratigraphic framework bounded by Maximum Flooding Surfaces. These units exhibit favorable stacking patterns, high net-to-gross ratios, and clean, coarsening-upward textures consistent with progradational deltaic deposition.

Key findings include:

- The identification of hybrid traps formed by structural closures and stratigraphic terminations against marine shales.
- The classification of reservoir units into HST, TST, and LST system tracts with variable petrophysical responses.
- Effective porosity (20–34%) and moderate permeability (2.5–18 mD) in most units, with LST sands demonstrating the highest reservoir quality.
- Hydrocarbon saturation patterns that reflect depositional environment, capillary behavior, and burial depth.
- Distinct structural compartments suitable for targeted development, supported by volumetric estimations and petrophysical trends.

The reservoir model developed in this work significantly reduces geological uncertainty and informs strategic field development plans, particularly for onshore marginal fields in mature basins. The workflow demonstrated here is applicable to similar deltaic systems globally, providing a reliable template for maximizing recovery in structurally and stratigraphically complex settings.

Acknowledgment

The authors sincerely thank the Department of Geology, Federal University of Technology Owerri, for providing an enabling environment and laboratory facilities that supported this research. We also acknowledge the Shell Petroleum Development Company (SPDC) and the Department of Petroleum Resources (DPR) for providing the dataset used for this study.

REFERENCES

- [1] Doust, H., Omatsola, E., Niger Delta. In: Edwards, J. D., Santogrossi, P.A. (Eds.), Divergent/passive margin basins, AAPG Memoir 48, 239–248, 1990.
- [2] Reijers T.J.A., Stratigraphy and sedimentology of the Niger Delta. *Geologos*, 17 (3): 133–162, 2011.
- [3] Anyanwu, T.C., Ekpo, B.O., Orji, B.A., Biomarker application in the recognition of the geochemical characteristics of crude oils from the five depobelts of the Niger Delta basin, Nigeria. *Iranian Journal of Earth Sciences*, 14(1):1-17, 2022.
- [4] Ebong, D.E., Akpan, A.E., Urang, J.G., 3D Structural modelling and fluid identification in parts of Niger Delta Basin, Southern Nigeria. *Journal of African Earth Sciences*, 158, 103565, 2019.
- [5] Amigun J.O., Bakare N.O., Reservoir evaluation of “Danna” field Niger Delta using petrophysical analysis and 3-D seismic interpretation. *Pet Coal* 2(55):119–127, 2013.
- [6] Galloway, W.E., Genetic stratigraphic sequences in basin analysis I: Architecture and genesis of flooding-surface bounded depositional units. *AAPG Bulletin*, 73(2), 125–142, 1989.
- [7] Cătuneanu O., *Principles of Sequence Stratigraphy*. Elsevier, Amsterdam. 2006.
- [8] Van Wagoner, J.C., Mitchum, R.M., Campion K.M., Rahmanian, V.D., *Siliciclastic Sequence Stratigraphy in Well Logs, Cores, and Outcrops*. American Association of Petroleum Geologists. *Methods in Exploration Series*, 7, 55 p., 1990.
- [9] Posamentier H.W., Allen G.P., *Siliciclastic sequence stratigraphy: concepts and applications*. *Concepts in Sedimentology and Paleontology*. SEPM Special Publication 7:210, 1999.
- [10] Reijers, T.J.A., Petters, S.W., Nwajide, C.S., The Niger Delta basin, in R.C. Selley, (ed), *African basins*. Amsterdam, Elsevier Science. *Sedimentary Basins of the World* 3:151–172, 1997.
- [11] Stacher P., Present understanding of the Niger delta hydrocarbon habitat, in Oti M.N., Postma G. (ed), *Geology of deltas*. Rotterdam, A.A. Balkema, 257–267, 1995.
- [12] Asquith, G., Krygowski, D., *Basic Well Log Analysis*. Vol. 16, American Association of Petroleum Geologists, Tulsa, 31-34, 2004.
- [13] Rider, M.H., Kennedy, M., *The Geological Interpretation of Well Logs*. Science, 432 p., 2011.
- [14] Worthington, P.F., Formation evaluation in horizontal wells- the pivotal role of anisotropy. *Petrophysics* 49(4):331–341, 2008.
- [15] Adegoke A. K., Sequence Stratigraphy of Some Middle to Late Miocene Sediments, Coastal Swamp Depobelts, Western Offshore Niger Delta. *International Journal of Science and Technology* 2 (1):18–28, 2012
- [16] Benkhelil, J., Structure and geodynamic evolution of the intracontinental Benue trough (Nigeria). *Elf Nig. Ltd., Nigeria Bull Centres Rech.Explor.Prod. Elf-Aquitaine (BCREDP)* 12:29–128, 1986.

- [17] Corredor F., Shaw J.H., Bilotti F., Structural styles in the deep-water fold and thrust belts of the Niger Delta. *American Association of Petroleum Geologists Bulletin* 89(6): 753–780, 2005.
- [18] Anyanwu T.C., Agbi I.O., Takyi B., Njoku J.O., Ugbaja U.A., Biological Marker Fingerprints of Crude Oils from Three Oilfields in the Central Niger Delta: Implication to Source Input, Conditions of Deposition, and Thermal Maturation. *GeoScience Engineering* 68: 134-150, 2022.
- [19] Anomneze, D.O., Okoro, A.U., Ajaegwu, N.E., Okeke, G.C., Description and interpretation of fault-related sedimentation and controls on shelf-edge deltas: Implication on sand transportation to the basin floor in parts of Eastern Niger Delta. *Journal of Petroleum Exploration and Production Technology*, 10(4), 1367–1388, 2020.
- [20] Anyanwu, T.C. Ekpo B.O., Petroleum system, filling history and age appraisal of source rocks of the Niger Delta Basin: Fingerprinting of pentacyclic triterpenoids. *Energy Geoscience*, 6:100399, 2025.
- [21] Short K.C., Stauble A.J., Outline of Geology of Niger delta. *American Association of Petroleum Geologists Bulletin* 51:761-779, 1967.
- [22] Anyanwu, T.C., Ekpo B.O., Orji, B.A., Geochemical Characterization of the Coastal and Offshore Niger Delta Crude Oils, Nigeria. *International Journal of Advanced Academic Research*, 7(12): 73-87, 2021.
- [23] Haq, B.U., Hardenbol, J., Vail, P.R., Mesozoic and Cenozoic chronostratigraphy and cycles of sea-level change. *Sea-Level Changes: An Integrated Approach*, SEPM Special Publication, 42, 71–108. 1988.
- [24] Onyekuru S.O., Ibelegbu E.C., Iwuagwu J.C., Essien A.G., Akaolisa C.Z., Sequence Stratigraphic Analysis of “XB Field”, Central Swamp Depobelt, Niger Delta Basin, Southern Nigeria. *International Journal of Geosciences* 3: 237-257, 2012.
- [25] Ukpong A.J., Anyanwu T.C., Osung W.E., Omoko E.N., Sequence Stratigraphic Study of B-24 Well Northern Depobelt, Niger Delta. Southeastern Nigeria, *Journal of Applied Geology and Geophysics* 6 (2): 20-28, 2018.
- [26] Onyekuru, S.O., Adumekwe, O.V., Ukpong, A.J., Ikoro, D.O., Anyanwu, T.C, Ofoh, I.J., Sequence stratigraphic interpretation of Middle–Late Miocene successions of OMAH–1 well Offshore Niger Delta, Nigeria. *Iranian Journal of Earth Science (IJES)*, 17(2), 1-14, 2025.
- [27] Tiab, D., Donaldson, E.C., *Petrophysics: Theory and Practice of Measuring Reservoir Rock and Fluid Transport Properties*. Gulf Professional Publishing, 2015.
- [28] Jones, S.C., Measuring the permeability of tight formations. *Journal of Petroleum Technology*, 40(11), 1309–1318. 1988.
- [29] Agbasi O.E., Sen S., Inyang N.J., Etuk S.E., Assessment of pore pressure, wellbore failure and reservoir stability in the Gabo field, Niger Delta, Nigeria – Implications for drilling and reservoir management”, *Journal of African Earth Sciences*, vol. 173, art. 104038. DOI: 10.1016/j.jafrearsci.2020.104038, 2021.
- [30] Adegoke S.O., Omatsola M.E., Salami M.B., Benthic Foraminifera Biofacies of the Niger Delta. *Maritime Sediments Special Publication* 1:279–292, 1976.

-
- [31] Njoku, J.O., Anyanwu, T.C., Ikoru, D.O., Soronnadi-Ononiwu, G.C., Acra, J.E., Okoli, E.A., Agoha, C.C., Biostratigraphic and sequence stratigraphic study of the Late Cretaceous–Paleogene succession in the Anambra Basin, Southeastern Nigeria: Insights from the Amama-1 and Bara-1 wells. *Journal of African Earth Sciences*, 230, 105741. 2025.
- [32] Van Wagoner, J.C., Mitchum, R.M., Campion, K.M., Rahmanian, V.D., An Overview of the Fundamentals of Sequence Stratigraphy and Key Definitions. *SEPM Special Publication* 42. 1988.
- [33] Petters, S.W., Okosun, E.A., Edet, A.E., Reservoir rock properties of the Niger Delta. *Journal of African Earth Sciences*, 74, 1–10. 2012.
- [34] Oluwajana, O.A., Ehinola, O.A., Okeugo, C.G., Adegoke, O., Modeling Hydrocarbon Generation Potentials of Eocene Source Rocks in the Agbada Formation, Northern Delta Depobelt, Niger Delta Basin, Nigeria”. *Journal of Petroleum Exploration and Production Technology*, 7(2):379-388. 2017.
- [35] Abdulkadir, M., Bamgbade, A.S., Comparative Analysis of Oil Production from Marginal Fields: A Case Study of a Marginal Field in Nigeria. *Journal of Petroleum Science and Engineering*, 177, 1123-1136. 2019.

Received: March 2026; Revised: April 2026; Accepted: April 2026; Published: April 2026